Science Advances

Supplementary Materials for

A hotspot for posttranslational modifications on the androgen receptor dimer interface drives pathology and resistance to antiandrogens

Andrea Alegre-Martí *et al.*

Corresponding author: Eva Estébanez-Perpiñá, evaestebanez@ub.edu;
Pablo Fuentes-Prior, fuentespriorpablo@gmail.com; Álvaro Aytes, aaytes@idibell.cat

This PDF file includes:

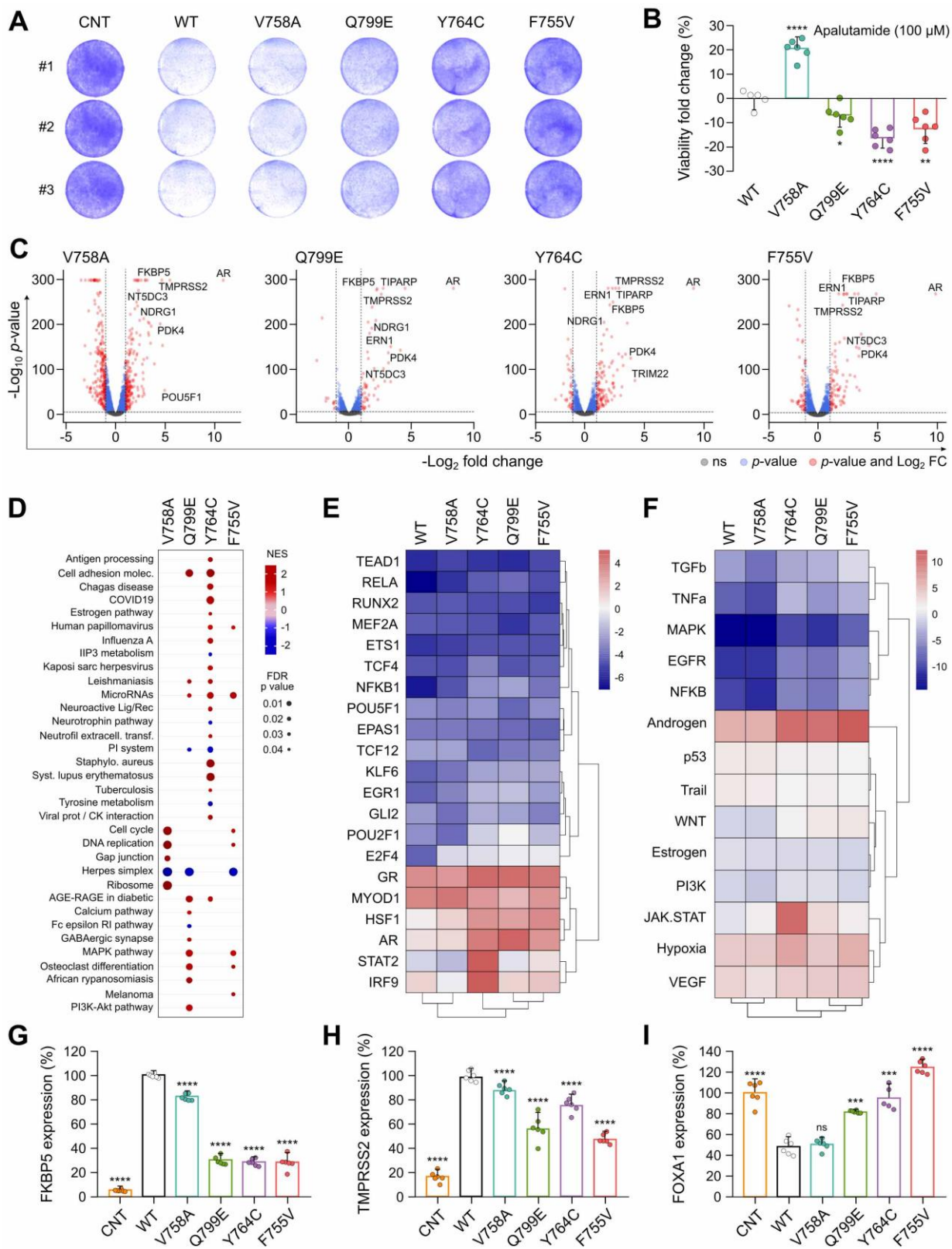Figs. S1 to S6
Tables S1 to S4
References

Fig. S1. The transcriptional profiles of AR-LBD dimerization surface mutants differ from that of the WT receptor.

Fig. S1 Legend. Summary of RNAseq experiments performed in triplicate for each cell line. **A,** Representative crystal violet-stained cultures used to quantitate the colony formation capacity of PC3 cells expressing WT or mutant AR. **B,** Relative viability fold change of CNT, WT, and mutant AR-transduced cells in response to the antiandrogen, apalutamide. **C,** Volcano plots showing the differential expression analysis between PC3-CNT and PC3-mut AR cells (V758A, Q799E, Y764C and F755V as indicated), using DESeq2 data. Genes with an absolute log2(fold change) ≥ 1 and a p value ≤ 0.05 are labeled in red. **D,** Analysis of the mutant AR signatures against WT AR on the KEEG Pathway database using GSEA. Note that the Y764C mutant is significantly enriched in pathways related to pathogen infection and immune response activation. Normalized Enrichment Score (NES) scale and False Discovery Rate (FDR) p value thresholds are indicated. **E,** Transcription factor regulon enrichment heatmap using DoRothEA. Regulons with an adjusted FDR p value ≤ 0.05 on the NES are shown. Note the strong enrichment of the STAT2 transcription factor in line with activation of the pathogen infection and inflammatory response pathways shown in (D). **F,** Pathway activity heatmap using the Pathway RespOnsive GENes for activity Inference (PROGENy) algorithm. In line with data shown in (D) and (E), the JAK/STAT pathway is significantly enriched in the Y764C mutant AR cells compared to both WT and other AR mutants. **G-H,** RT-qPCR validation of AR transcriptional activity using canonical targets FKBP5 (**G**) and TMPRSS2 (**H**). Also shown is the RT-qPCR validation for expression of the pioneer factor, FOXA1, in WT and mutant AR transduced cells (**I**). RT-qPCR measurements were conducted in triplicate (mean $\pm$ SD are shown) and differences against WT-AR cells were calculated using a t-test and considered significant at p values < 0.05. (*$p < 0.05$, ** $p < 0.01$, *** $p < 0.001$ and **** $p < 0.0001$).
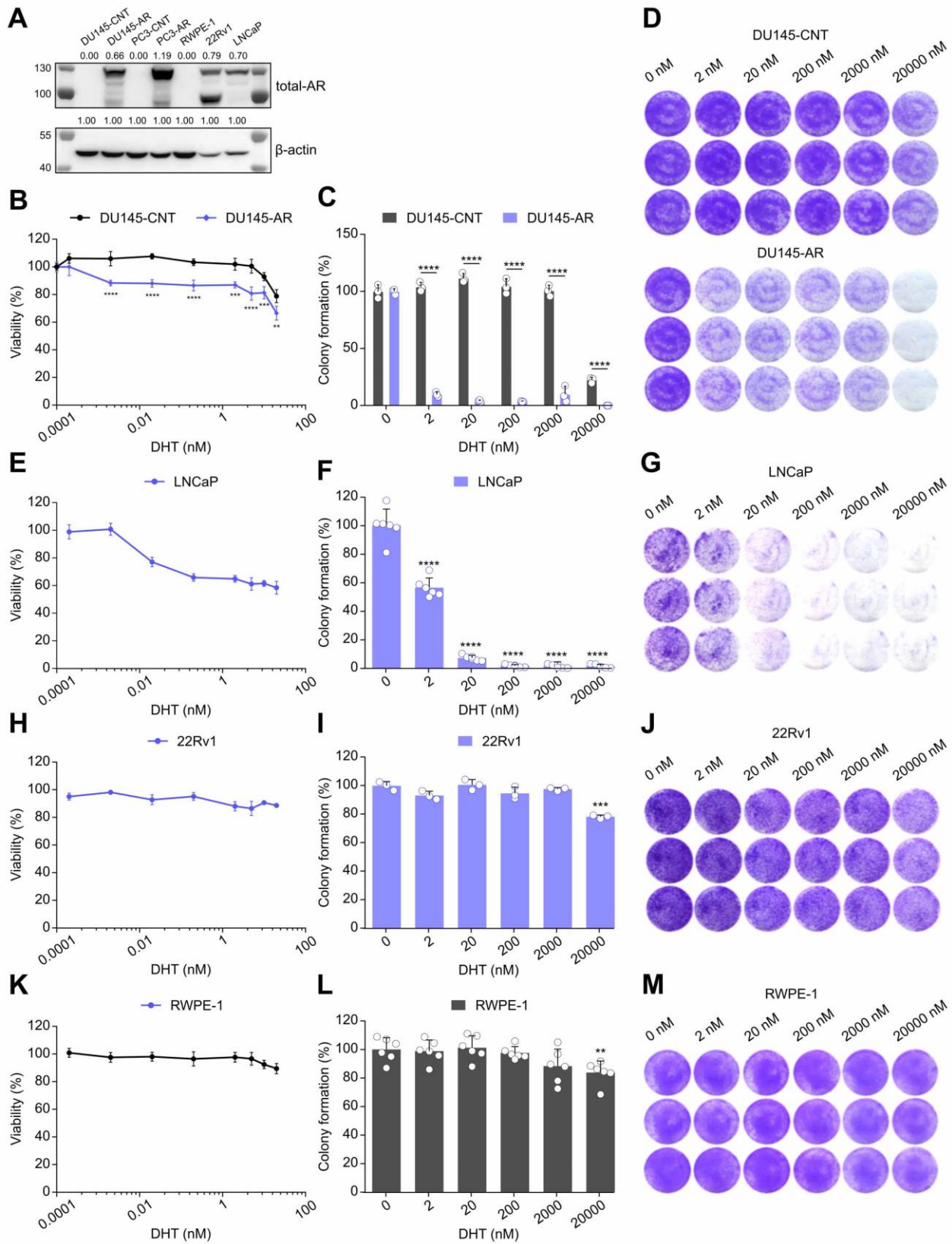
Fig. S2. Supraphysiological DHT concentrations suppress cell growth of AR-responsive cell lines.

Fig. S2 Legend. A, Western blot analysis of total AR in the cell lines and derivatives used in the current study. **B to D,** Analysis of the effect of AR expression in DU145 cells. **B,** Viability assays comparing parental and AR-expressing cells upon DHT treatment. **C and D**, Quantification and representative images of colony formation assays in parental and AR-expressing DU145 cells. Note the significant reduction in viability and clonogenicity in AR-expressing cells upon DHT stimulation. **E to G**, Analysis of the effect of AR expression in LNCaP cells. **E**, Viability assay of LNCaP cells upon DHT treatment. **F and G,** Quantification and representative images of colony formation assays in LNCaP cells. **H to J,** Analysis of the effect of AR expression in CRPC 22Rv1 cells**. H,** viability assays of 22Rv1 in response to DHT treatment. **I and J**, Quantification and representative images of colony formation assays in 22Rv1 cells. Note that 22Rv1 cells express the truncated AR variant lacking the LBD and therefore do not respond to DHT. **K to M,** Analysis of the effect of AR activation upon DHT treatment in AR-negative RWPE-1 cells. **K,** Viability assays of RWPE-1 cells upon DHT treatment. **L and M**, Quantification and representative images of colony formation assays in RWPE-1 cells. Note that in RWPE-1 cells do not express AR and similarly to parental PC3 and DU145 cells do not respond to DHT. Viability and clonogenic assays were conducted in n=3 or n=6 as indicated (mean ± SD are shown) and differences were calculated using a t-test and considered significant at p values < 0.05. (*$p < 0.05$, **$p < 0.01$, ***$p < 0.001$ and ****$p < 0.0001$).
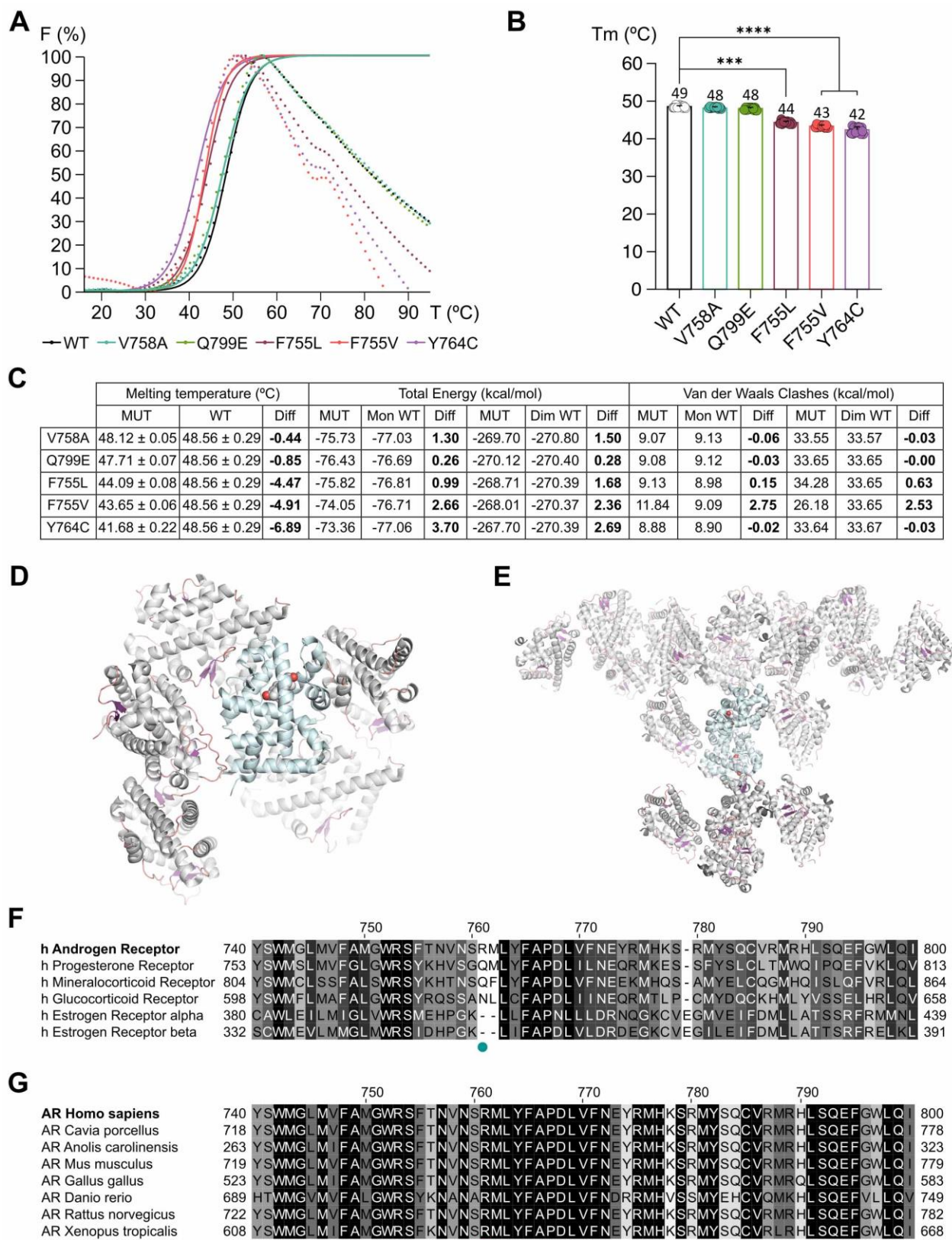
Fig. S3. In solution and *in silico* characterization of AR-LBD dimer interface mutants.

Panel C table:

	Melting temperature (°C)			Total Energy (kcal/mol)						Van der Waals Clashes (kcal/mol)					
	MUT	WT	Diff	MUT	Mon WT	Diff	MUT	Dim WT	Diff	MUT	Mon WT	Diff	MUT	Dim WT	Diff
V758A	48.12 ± 0.05	48.56 ± 0.29	**-0.44**	-75.73	-77.03	**1.30**	-269.70	-270.80	**1.50**	9.07	9.13	**-0.06**	33.55	33.57	**-0.03**
Q799E	47.71 ± 0.07	48.56 ± 0.29	**-0.85**	-76.43	-76.69	**0.26**	-270.12	-270.40	**0.28**	9.08	9.12	**-0.03**	33.65	33.65	**-0.00**
F755L	44.09 ± 0.08	48.56 ± 0.29	**-4.47**	-75.82	-76.81	**0.99**	-268.71	-270.39	**1.68**	9.13	8.98	**0.15**	34.28	33.65	**0.63**
F755V	43.65 ± 0.06	48.56 ± 0.29	**-4.91**	-74.05	-76.71	**2.66**	-268.01	-270.37	**2.36**	11.84	9.09	**2.75**	26.18	33.65	**2.53**
Y764C	41.68 ± 0.22	48.56 ± 0.29	**-6.89**	-73.36	-77.06	**3.70**	-267.70	-270.39	**2.69**	8.88	8.90	**-0.02**	33.64	33.67	**-0.03**

Fig. S3 Legend. A and B, Thermal shift assay of purified WT and mutant AR-LBDs. The melting curves of each sample **(A)** were analyzed to calculate their melting temperatures **(B)** (mean ± SD, n = 4). Differences against WT AR-LBD were calculated using the t-test and considered significant at p values < 0.05. (*p < 0.05, ** p < 0.01, *** p < 0.001 and **** p < 0.0001). **C,** Comparison between the experimentally determined melting temperatures (B) and the *in silico* calculated free energies of unfolding and Van der Waals clashes with FoldX. **D and E,** Crystal packing in monomeric (**D**, PDB 1T7T) and tetrameric AR-LBD (**E**, PDB 5JJM). Only the closest crystal neighbors are shown. **F and G,** Partial sequence alignments of the AR-LBD sequence around residue Arg761 (marked with a blue dot). Residues topologically equivalent to the Tyr740-Ile800 sequence of human AR are compared to other steroid receptors (**F**) and to AR sequences from different species (from fish to humans; **G**). Strictly conserved residues are white with black shading; other conservative mutations are colored by conservation (the darker, the more conserved). Note that Arg761 is strictly conserved among the different species of AR, but not in other steroid receptors.
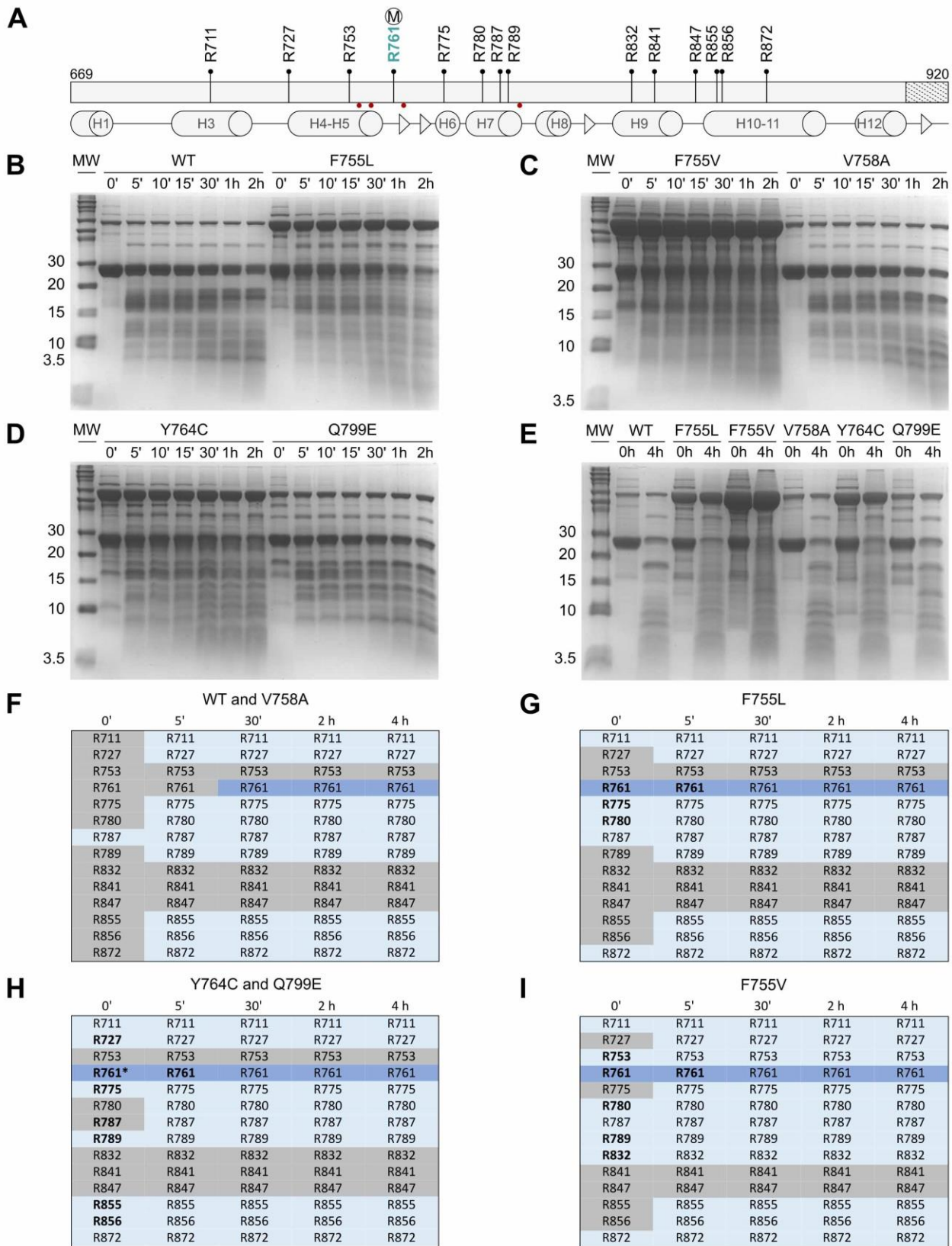
Fig. S4. AR-LBD interface residue mutations alter sensitivity to proteolysis of the domain.

Fig. S4 Legend. A, Schematic representation of the AR-LBD secondary structure. The positions of the 14 arginine residues within the domain are indicated; the methylated Arg761 is labeled in blue (M). Red dots mark the position of the mutated residues in the current investigation. **B to D,** Representative SDS-polyacrylamide gels showing the time course of proteolytic cleavage of WT and mutant AR-LBDs with Arg-C. **E,** SDS-PAGE analysis of initial and end time points (limited proteolysis with Arg-C for 4 h). **F to I,** Inferred proteolysis patterns for each mutant. Uncleaved arginines are shown in gray, cleaved Arg761 is colored dark blue, and other cleaved arginines in sky blue. Bold-labeled arginines are cleaved with different kinetics compared to WT AR-LBD. Note that four different proteolysis patterns can be observed, corresponding to (F) WT and V758A, (G) F755L, (H) Y764C and Q799E, and (I) F755V.
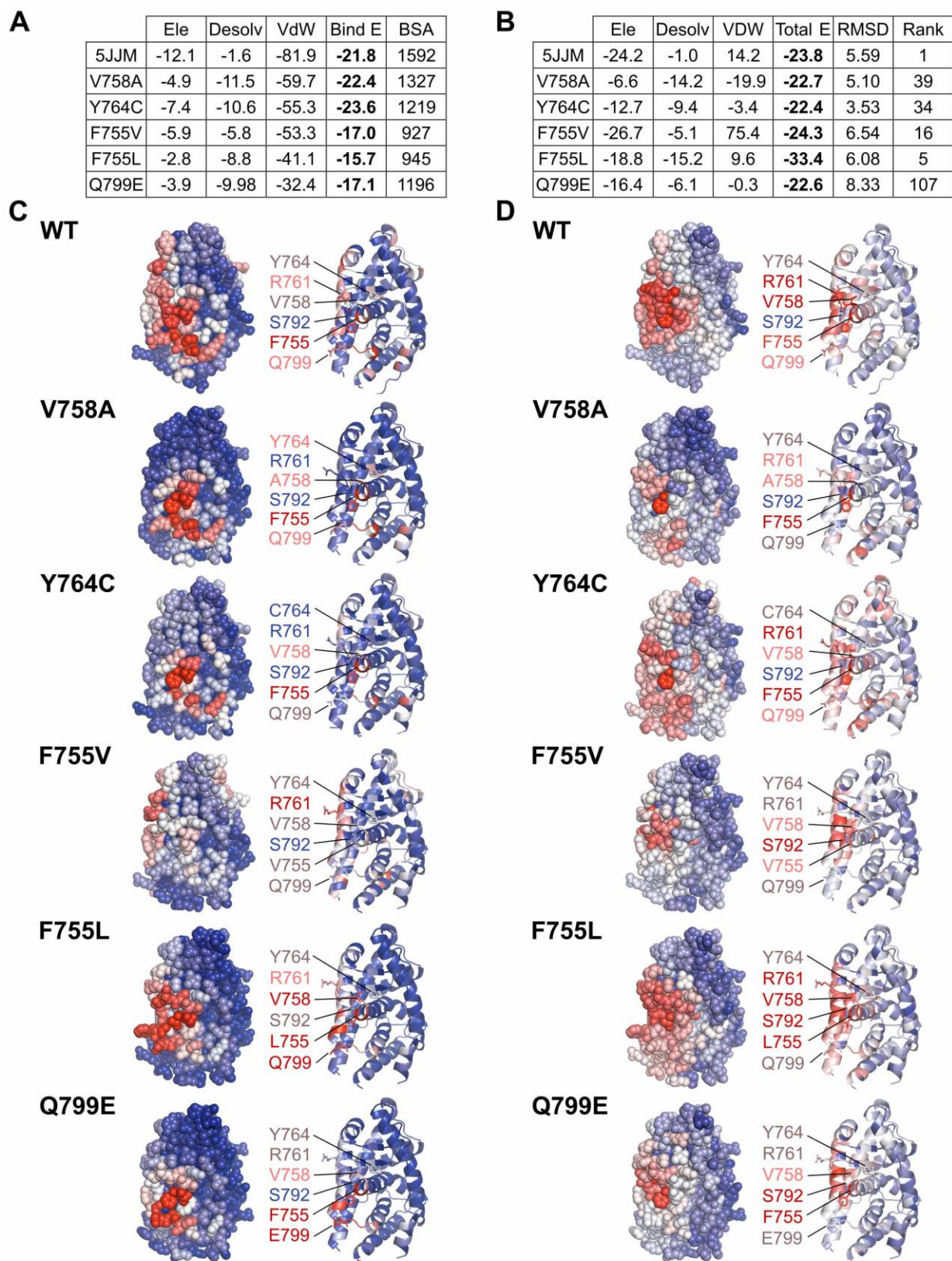
A

	Ele	Desolv	VdW	Bind E	BSA
5JJM	-12.1	-1.6	-81.9	**-21.8**	1592
V758A	-4.9	-11.5	-59.7	**-22.4**	1327
Y764C	-7.4	-10.6	-55.3	**-23.6**	1219
F755V	-5.9	-5.8	-53.3	**-17.0**	927
F755L	-2.8	-8.8	-41.1	**-15.7**	945
Q799E	-3.9	-9.98	-32.4	**-17.1**	1196

B

	Ele	Desolv	VDW	Total E	RMSD	Rank
5JJM	-24.2	-1.0	14.2	**-23.8**	5.59	1
V758A	-6.6	-14.2	-19.9	**-22.7**	5.10	39
Y764C	-12.7	-9.4	-3.4	**-22.4**	3.53	34
F755V	-26.7	-5.1	75.4	**-24.3**	6.54	16
F755L	-18.8	-15.2	9.6	**-33.4**	6.08	5
Q799E	-16.4	-6.1	-0.3	**-22.6**	8.33	107

Fig. S5. AR-LBD interface mutants are predicted to dimerize essentially as non-canonical WT AR-LBD.

Fig. S5 Legend. A, Buried surface area (BSA) and pyDock scoring (total binding energy, calculated as the sum of electrostatics (Ele), desolvation (Dslvt), and one-tenth of the VdW energy term) for dimeric AR-LBD. Values were calculated assuming that mutants dimerize as in the previously reported structure of WT AR-LBD (B:C chains of PDB entry 5JJM). **B,** pyDock scoring of the best-ranked docking solutions. Docking experiments with WT AR-LBD (B chain from 5JJM) and the current structures of monomeric mutant with themselves were independently conducted. In all cases, arrangements close to the experimental dimer were identified among the top solutions (RMSD < 10 Å). **C,** Hotspot interface residues in WT and mutant AR-LBD predicted from docking experiments. Surface residues are colored according to their normalized interface propensity (NIP), from lowest (blue) to highest (red) values; intermediate values are scaled accordingly (left panel). Residues of interest are labeled and colored according to their relative NIP values in the right panel. **D,** Predicted protein-protein interaction optimal docking areas (ODA). Residues are colored according to their ODA values, from minimum (red) to maximum (blue), and intermediate values are scaled accordingly (left panel). Residues of interest are labeled and colored according to their relative ODA values (right panel).
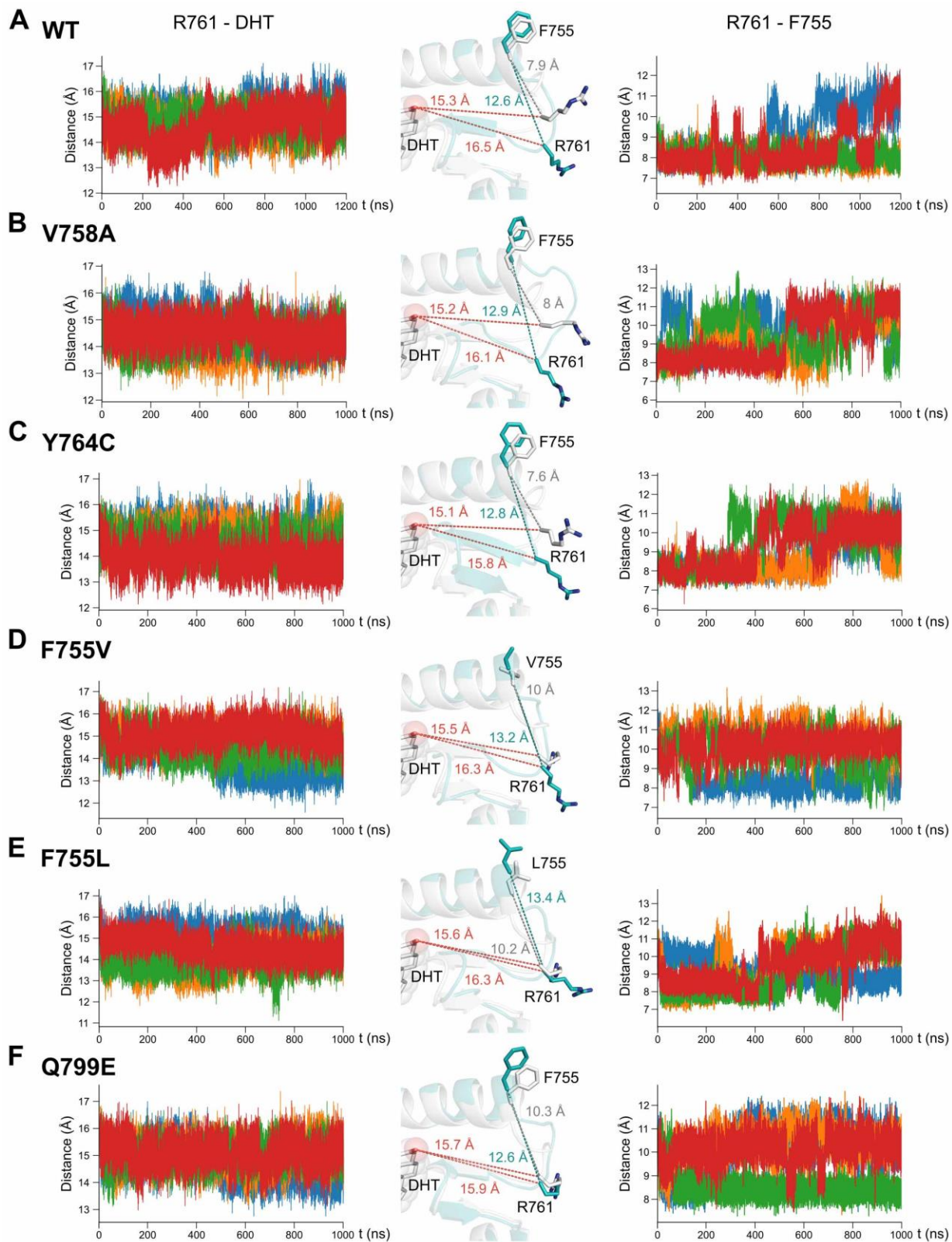
Fig. S6. Dynamics of R761-zone large conformational reorientations.

Fig. S6 Legend. Molecular dynamics were performed in quadruplicate. **A-F,** Analysis of the displacements of the H5-S1 loop along the MD simulations, as assessed by the time evolution of the distances between the Cα atoms of some of the most significant pairwise interactions identified from the inter-residue distance calculations, represented in the left and right panels of each AR-LBD row, respectively (see Materials and Methods section for details). Figures in the central panels represent the calculated distances between Arg761 and DHT (in red) or mutated residues (Phe755, Val758 and Tyr764) for the AR-LBD WT structure and mutants. Minimum and maximum distances identified during the MD simulations are colored gray and blue, respectively, to illustrate the dynamical changes of the H5-S1 loop.

LBP			AF-2			BF-3			Dimer interface			R761-zone			Arginines		
Res	PCa	AIS	Res	PCa	AIS	Res	PCa	AIS	Res	PCa	AIS	Res	PCa	AIS	Res	PCa	AIS
L702	H	I	L713		F	I673	T		P672		H, S	W752	C	R	R711	G, I	T
L705			V714			F674		C	L675	R, P		F755	L	V, L, S	R727	C, H, L	
N706	S	S, Y, I	V717		F	P724	T	S, L	E679	K	G	T756	A		R753	Q	Q, P
L708		R	K718			G725	D	S, A, V	A680	T, G		N757	D, S, K	S	R761	G	S
G709		R	K721		L	R727	M		E682	K, V, D	K, D	V758	I, L, A		R775	C, H	C, H
Q712		E	F726	C, H, L		N728		K	P683	S, L	T, A	N759		T	R780	G, Q	W
W742	L, C	R	R727	M		F827	L	L	G684			S760	P	F, Y	R787	Q	
M743		V	V731	H	H	E830	K, D		V685	A	I	R761		S	R789		S
M746		T, I, L	Q734			L831	P	V	C687		R	Y764	C	C, H	R832	Q	Q, L
V747		M	M735		F, T	N834			W752	C	R	R789		S	R841	C, H, L	C, G, H, S
M750	T, K, I	V	I738		R	E838			R753			H790	Q		R847	G	
R753	Q	Q, P	Q739	K		R841	C, H, L	C, H, G, S	F755	L	V, L, S	S792	P, F		R855		K
F765		L	E894						T756	A		Q793			R856	C, H	C, H
M781		I	M895	D	G				N757	D, S, K		W797			R872		G
M788	I		E898		F, T				V758	I, L, A		Q799	E	E			
L874			I899						N759		T						
H875	Y, Q	R							R761		S						
F877	L								M762		T						
T878	A, S	I							Y764	C	H, C						
L881	Q								P767	T	S, A						
M896	L	T							D768	N	E, Y						
									G796	E, V							
									Q799	E	E						
									I800	T							
									T801		I						
									P802	L							
									Q803		R						
									L806								
									C845								
									K846								
									R847	G							
									K848	N							
									N849	H, K	K						
									S852								
Total residues	21			16			12			34			15			14		
Mutated residues	19	11	16	11	5	8	10	8	7	25	21	18	13	10	9	14	10	11
Unique mutations	35	16	21	16	7	10	21	11	13	51	32	27	24	15	13	28	18	18

Table S1. Reported mutations in the major functional areas of the AR-LBD.

Mutations that affect the ligand-binding pocket (LBP) as well as the major protein-protein interaction sites, AF-2, BF-3 and the dimer interface are separately given. Within each subgroup, we also distinguish between those reported in PCa patients and in AIS cases. The total numbers of mutated residues and of unique mutations within each functional region are given at the bottom of the table. Note that several mutations have been linked to both PCa and AIS (e.g., R753Q, F755L).

Mutant	Identified in	Protein stability	Ligand affinity	Intra- and intermolecular interactions	Transcriptional activity	Ref.
F755V	CAIS	Not studied	Five-fold lower affinity for mibolerone.	Reduced N/C interaction.	Largely impaired (5% of WT activity at 10 nM DHT).	(35, 37)
F755L	PCa, PAIS	Enhanced thermolability but as resistant to trypsinolysis as WT protein.	One-third of the affinity for DHT and mibolerone. 10-fold higher concentration of androgen needed to achieve same activity as WT.	Severely compromised N/C interactions. Reduced binding to Qia2.	Significantly impaired: high activity with mibolerone and methyltrienolone, 40-60% of WT with DHT, 30% of WT activity with testosterone.	(37, 39, 54, 59, 60, 61)
V758A	PCa	Not studied	PC3 transiently expressing AR V758A present sensitivity to darolutamide.	Increased binding to coactivators and impaired binding to corepressors. WT-like or increased N/C interaction.	Normal activity in response to DHT; weak activity with DHEA.	(38, 39, 40, 41, 42)
R761G	PCa	Not studied	Not studied	Not studied	Poor response to low concentrations of R1881 in CV-1 cells, but WT-like activity in PC3 cells. EPI-002 inhibitor blocks mutant activity similar to WT.	(62, 121, 122)
Y764C	PCa, PAIS	More thermolabile, especially in combination with a shorter polyQ stretch.	WT-like binding to DHT, but reduced binding to other androgens, non-androgens, and anti-androgens.	Abnormal or even complete loss of N/C interactions.	Conflicting results: reported to have complete, moderate, or no function at all in different studies.	(32, 39, 42, 43, 44, 46, 48)
Q799E	PCa, PAIS	Normal thermal stability.	Normal androgen binding. Sensitive to darolutamide in PC3 cells.	Mild reduction of N/C interaction. Reduced binding to Qia2. Impaired binding to NCoA.	Impaired at normal androgen doses but overcome with high doses. In other studies, full activity in the presence of DHT an partial activity DHEA.	(39, 42, 48, 49, 50, 51, 52, 54)

Table S2. Summary of clinical and biological information on point mutants that affect the AR-LBD dimerization interface.

AR-LBD(Y764C) Cys-Cys covalent bound peptides								
Site A	Site B	Sequence A	Sequence B	MeroX	XlinkX	Xi SEARCH	Max among Nodes	Stars
C-687	C-764	^{680}AIEPGVVCAGHDNNQPDSFAALLSSLNE^{707}	^{762}MLCFAPDLVFNE^{773}	5	3	2	5	***
		^{680}AIEPGVVCAGHDNNQPDSFAALLSSLNE^{707}	^{762}MLCFAPDLVFNEYR^{773}	1	9	4	9	***
	C-785	^{680}AIEPGVVCAGHDNNQPDSFAALLSSLNE^{707}	^{781}MYSQCVR^{787}			1	1	*
	C-807	^{680}AIEPGVVCAGHDNNQPDSFAALLSSLNE^{707}	^{795}FGWLQITPQEFLCMK^{809}	2	2	2	2	***
	C-853	^{680}AIEPGVVCAGHDNNQPD^{696}	^{849}NPTSCSR^{855}			1	1	*
		^{680}AIEPGVVCAGHDNNQPDSFAALLSSLNE^{707}	^{849}KNPTSCSR^{855}			1	1	*
			^{849}NPTSCSR^{855}			1	1	*
C-764	C-764	^{762}MLCFAPDLVFNE^{773}	^{762}MLCFAPDLVFNEYR^{775}			2	2	*
		^{762}MLCFAPDLVFNEYR^{775}	^{762}MLCFAPDLVFNE^{733}		1		1	*
			^{762}MLCFAPDLVFNEYR^{775}	7		4	7	**
	C-785	^{762}MLCFAPDLVFNE^{773}	^{781}MYSQCVR^{787}		2	3	3	**
		^{762}MLCFAPDLVFNEYR^{775}	^{781}MYSQCVR^{787}		14	6	14	**
	C-807	^{762}MLCFAPDLVFNE^{773}	^{795}FGWLQITPQEFLCMK^{809}			1	1	*
		^{762}MLCFAPDLVFNEYR^{775}	^{795}FGWLQITPQEFLCMK^{809}	3	7	4	7	***
	C-845	^{762}MLCFAPD^{768}	^{842}IIACK^{846}		1		1	*
		^{762}MLCFAPDLVFNE^{773}	^{842}IIACK^{846}	1	1		1	**
		^{762}MLCFAPDLVFNEYR^{775}	^{842}IIACK^{846}		8		8	*
	C-853	^{762}MLCFAPD^{768}	^{849}NPTSCSR^{855}		1	2	2	**
		^{762}MLCFAPDLVFNE^{773}	^{849}NPTSCSR^{855}			1	1	*
		^{762}MLCFAPDLVFNEYR^{775}	^{848}KNPTSCSR^{855}		1	1	1	**
			^{849}NPTSCSR^{855}		5	4	5	**

Table S3. Summary of Cys-Cys' covalently linked peptides in the covalent AR-LBD(Y764C) dimer identified by mass spectrometry.

The sequences of disulfide-bridged tryptic peptides identified in samples of dimeric Y764C are given along with the number of counts each peptide pair was detected with different software.

AR-LBD(Y764C) Cys-Cys crosslinked with BMB								
Site A	Site B	Sequence A	Sequence B	MeroX	XlinkX	Xi SEARCH	Unique CSM	Stars
C-764	C-764	^{762}MLCFAPDLVFNEYR^{775}	^{762}MLCFAPDLVFNEYR^{775}	5		5	8	**
	C-785	^{762}MLCFAPDLVFNEYR^{775}	^{781}MYSQCVR^{787}		6	5	9	**
	C-853	^{762}MLCFAPDLVFNEYR^{775}	^{849}NPTSCSR^{855}		1	2	3	**

Table S4. Summary of BMB-crosslinked peptides in the covalent AR-LBD(Y764C) dimer identified by mass spectrometry. The number of counts each peptide pair was detected with different search tools is indicated. The only BMB-crosslinked tryptic peptides identified by MS involve the mutant Cys764, demonstrating its higher reactivity in solution.

REFERENCES AND NOTES

1. W. D. Tilley, C. M. Wilson, M. Marcelli, M. J. McPhaul, Androgen receptor gene expression in human prostate carcinoma cell lines. *Cancer Res.* **17**, 5382–5386 (1990).

2. E. Estébanez-Perpiñá, C. L. Bevan, I. J. McEwan, Eighty years of targeting androgen receptor activity in prostate cancer: The fight goes on. *Cancers* **13**, 509 (2021).

3. A. Jiménez-Panizo, P. Pérez, A. M. Rojas, P. Fuentes-Prior, E. Estébanez-Perpiñá, Non-canonical dimerization of the androgen receptor and other nuclear receptors: Implications for human disease. *Endocr. Relat. Cancer* **26**, R479–R497 (2019).

4. X. Yu, P. Yi, R. A. Hamilton, H. Shen, M. Chen, C. E. Foulds, M. A. Mancini, S. J. Ludtke, Z. Wang, B. W. O'Malley, Structural insights of transcriptionally active, full-length androgen receptor coactivator complexes. *Mol. Cell* **79**, 812–823.e4 (2020).

5. P. L. Shaffer, A. Jivan, D. E. Dollins, F. Claessens, D. T. Gewirth, Structural basis of androgen receptor binding to selective androgen response elements. *Proc. Natl. Acad. Sci. U.S.A.* **101**, 4758–4763 (2004).

6. M. Nadal, S. Prekovic, N. Gallastegui, C. Helsen, M. Abella, K. Zielinska, M. Gay, M. Vilaseca, M. Taulès, A. B. Houtsmuller, M. E. van Royen, F. Claessens, P. Fuentes-Prior, E. Estébanez-Perpiñá, Structure of the homodimeric androgen receptor ligand-binding domain. *Nat. Commun.* **8**, 14388 (2017).

7. E. V. Wasmuth, A. Vanden Broeck, J. R. LaClair, E. A. Hoover, K. E. Lawrence, N. Paknejad, K. Pappas, D. Matthies, B. Wang, W. Feng, P. A. Watson, J. C. Zinder, W. R. Karthaus, M. J. de la Cruz, R. K. Hite, K. Manova-Todorova, Z. Yu, S. T. Weintraub, S. Klinge, C. L. Sawyers, Allosteric interactions prime androgen receptor dimerization and activation. *Mol. Cell.* **82**, 2021–2031 (2022).

8. K. E. Knudsen, T. M. Penning, Partners in crime: Deregulation of AR activity and androgen synthesis in prostate cancer. *Trends Endocrinol. Metab.* **21**, 315–324 (2010).

9. Y. Wen, M. C.-T. Hu, K. Makino, B. Spohn, G. Bartholomeusz, D. H. Yan, M. C. Hung, HER-2/neu promotes androgen-independent survival and growth of prostate cancer cells through the Akt pathway. *Cancer Res.* **60**, 6841–6845 (2000).

10. H. K. Lin, S. Yeh, H. Y. Kang, C. Chang, Akt suppresses androgen-induced apoptosis by phosphorylating and inhibiting androgen receptor. *Proc. Natl. Acad. Sci. U.S.A.* **98**, 7200–7205 (2001).

11. H. K. Lin, Y. C. Hu, L. Yang, S. Altuwaijri, Y. T. Chen, H. Y. Kang, C. Chang, Suppression Versus Induction of androgen receptor functions by the phosphatidylinositol 3-Kinase/Akt pathway in prostate cancer LNCaP cells with different passage numbers. *J. Biol. Chem.* **278**, 50902–50907 (2003).

12. S. S. Taneja, S. Ha, N. K. Swenson, H. Y. Huang, P. Lee, J. Melamed, E. Shapiro, M. J. Garabedian, S. K. Logan, Cell-specific regulation of androgen receptor phosphorylation in vivo. *J. Biol. Chem.* **280**, 40916–40924 (2005).

13. K. Xu, H. Shimelis, D. E. Linn, R. Jiang, X. Yang, F. Sun, Z. Guo, H. Chen, W. Li, H. Chen, X. Kong, J. Melamed, S. Fang, Z. Xiao, T. D. Veenstra, Y. Qiu, Regulation of Androgen Receptor Transcriptional Activity and Specificity by RNF6-Induced Ubiquitination. *Cancer Cell* **15**, 270–282 (2009).

14. D. E. Linn, X. Yang, Y. Xie, A. Alfano, D. Deshmukh, X. Wang, H. Shimelis, H. Chen, W. Li, K. Xu, M. Chen, Y. Qiu, Differential regulation of androgen receptor by PIM-1 kinases via phosphorylation-dependent recruitment of distinct ubiquitin E3 ligases. *J. Biol. Chem.* **287**, 22959–22968 (2012).

15. D. Gioeli, B. M. Paschal, Post-translational modification of the androgen receptor. *Mol. Cell. Endocrinol.* **352,** 70–78 (2012).

16. T. van der Steen, D. J. Tindall, H. Huang, Posttranslational modification of the androgen receptor in prostate cancer. *Int. J. Mol. Sci.* **14**, 14833–14859 (2013).

17. Y. Koryakina, H. Q. Ta, D. Gioeli, Androgen receptor phosphorylation: Biological context and functional consequences. *Endocr. Relat. Cancer* **21**, T131–T145 (2014).

18. Z. Mounir, J. M. Korn, T. Westerling, F. Lin, C. A. Kirby, M. Schirle, G. McAllister, G. Hoffman, N. Ramadan, A. Hartung, Y. Feng, D. R. Kipp, C. Quinn, M. Fodor, J. Baird, M. Schoumacher, R. Meyer, J. Deeds, G. Buchwalter, T. Stams, N. Keen, W. R. Sellers, M. Brown, R. A. Pagliarini, ERG signaling in prostate cancer is driven through PRMT5-dependent methylation of the androgen receptor. *eLife* **5**, e13964 (2016).

19. L. Malbeteau, H. T. Pham, L. Eve, M. R. Stallcup, C. Poulard, M. Le Romancer, How protein methylation regulates steroid receptor function. *Endocr. Rev.* **43**, 160–197 (2022).

20. Q. Wang, W. Li, X. S. Liu, J. S. Carroll, O. A. Jänne, E. K. Keeton, A. M. Chinnaiyan, K. J. Pienta, M. Brown, A hierarchical network of transcription factors governs androgen receptor-dependent prostate cancer growth. *Mol. Cell* **27**, 380–392 (2007).

21. D. Robinson, E. M. Van Allen, Y. M. Wu, N. Schultz, R. J. Lonigro, J. M. Mosquera, B. Montgomery, M. E. Taplin, C. C. Pritchard, G. Attard, H. Beltran, W. Abida, R. K. Bradley, J. Vinson, X. Cao, P. Vats, L. P. Kunju, M. Hussain, F. Y. Feng, S. A. Tomlins, K. A. Cooney, D. C. Smith, C. Brennan, J. Siddiqui, R. Mehra, Y. Chen, D. E. Rathkopf, M. J. Morris, S. B. Solomon, J. C. Durack, V. E. Reuter, A. Gopalan, J. Gao, M. Loda, R. T. Lis, M. Bowden, S. P. Balk, G. Gaviola, C. Sougnez, M. Gupta, E. Y. Yu, E. A. Mostaghel, H. H. Cheng, H. Mulcahy, L. D. True, S. R. Plymate, H. Dvinge, R. Ferraldeschi, P. Flohr, S. Miranda, Z. Zafeiriou, N. Tunariu, J. Mateo, R. Perez-Lopez, F. Demichelis, B. D. Robinson, M. Schiffman, D. M. Nanus, S. T. Tagawa, A. Sigaras, K. W. Eng, O. Elemento, A. Sboner, E. I. Heath, H. I. Scher, K. J. Pienta, P. Kantoff, J. S. De Bono, M. A. Rubin, P. S. Nelson, L. A. Garraway, C. L. Sawyers, A. M. Chinnaiyan, Integrative clinical genomics of advanced prostate cancer. *Cell* **161**, 1215–1228 (2015).

22. D. A. Quigley, H. X. Dang, S. G. Zhao, P. Lloyd, R. Aggarwal, J. J. Alumkal, A. Foye, V. Kothari, M. D. Perry, A. M. Bailey, D. Playdle, T. J. Barnard, L. Zhang, J. Zhang, J. F. Youngren, M. P. Cieslik, A. Parolia, T. M. Beer, G. Thomas, K. N. Chi, M. Gleave, N. A. Lack, A. Zoubeidi, R. E. Reiter, M. B. Rettig, O. Witte, C. J. Ryan, L. Fong, W. Kim, T. Friedlander, J. Chou, H. Li, R. Das, H. Li, R. Moussavi-Baygi, H. Goodarzi, L. A. Gilbert, P. N. Lara, C. P. Evans, T. C. Goldstein, J.

M. Stuart, S. A. Tomlins, D. E. Spratt, R. K. Cheetham, D. T. Cheng, K. Farh, J. S. Gehring, J. Hakenberg, A. Liao, P. G. Febbo, J. Shon, B. Sickler, S. Batzoglou, K. E. Knudsen, H. H. He, J. Huang, A. W. Wyatt, S. M. Dehm, A. Ashworth, A. M. Chinnaiyan, C. A. Maher, E. J. Small, F. Y. Feng, Genomic Hallmarks and Structural Variation in Metastatic Prostate Cancer. *Cell*. **174**, 758–769.e9 (2018).

23. D. B. Lubahn, T. R. Brown, J. A. Simental, H. N. Higgs, C. J. Migeon, E. M. Wilson, F. S. French, Sequence of the intron/exon junctions of the coding region of the human androgen receptor gene and identification of a point mutation in a family with complete androgen insensitivity. *Proc. Natl. Acad. Sci. U.S.A.* **86**, 9534–9538 (1989).

24. O. Hiort, G. H. Sinnecker, P. M. Holterhus, E. M. Nitsche, K. Kruse, The clinical and molecular spectrum of androgen insensitivity syndromes. *Am. J. Med. Genet.* **63**, 218–222 (1996).

25. I. A. Hughes, J. D. Davies, T. I. Bunch, V. Pasterski, K. Mastroyannopoulou, J. Macdougall, Androgen insensitivity syndrome. *Lancet* **380**, 1419–1428 (2012).

26. C. E. Bohl, W. Gao, D. D. Miller, C. E. Bell, J. T. Dalton, Structural basis for antagonism and resistance of bicalutamide in prostate cancer. *Proc. Natl. Acad. Sci. U.S.A.* **102**, 6201–6206 (2005).

27. C. E. Bohl, Z. Wu, D. D. Miller, C. E. Bell, J. T. Dalton, Crystal structure of the T877A human androgen receptor ligand-binding domain complexed to cyproterone acetate provides insight for ligand-induced conformational changes and structure-based drug design. *J. Biol. Chem.* **282**, 13648–13655 (2007).

28. J. S. Sack, K. F. Kish, C. Wang, R. M. Attar, S. E. Kiefer, Y. An, G. Y. Wu, J. E. Scheffler, M. E. Salvati, J. Krystek, R. Weinmann, H. M. Einspahr, Crystallographic structures of the ligand-binding domains of the androgen receptor and its T877A mutant complexed with the natural agonist dihydrotestosterone. *Proc. Natl. Acad. Sci. U.S.A.* **98**, 4904–4909 (2001).

29. B. Gottlieb, L. K. Beitel, A. Nadarajah, M. Paliouras, M. Trifiro, The androgen receptor gene mutations database: 2012 update. *Hum. Mutat.* **33**, 887–894 (2012).

30. Z. Culig, A. Hobisch, M. Erdel, G. Bartsch, H. Klocker, Studies on androgen receptor mutations and amplification in human prostate cancer. *Methods Mol. Med.* **81**, 267–275 (2003).

31. E. R. Hyytinen, K. Haapala, J. Thompson, I. Lappalainen, M. Roiha, I. Rantala, H. J. Helin, O. A. Jänne, M. Vihinen, J. J. Palvimo, P. A. Koivisto, Pattern of somatic androgen receptor gene mutations in patients with hormone-refractory prostate cancer. *Lab. Invest.* **82**, 1591–1598 (2002).

32. M. J. McPhaul, M. Marcelli, W. D. Tilley, J. E. Griffin, R. F. Isidro-Gutierrez, J. D. Wilson, Molecular basis of androgen resistance in a family with a qualitative abnormality of the androgen receptor and responsive to high-dose androgen therapy. *J. Clin. Invest.* **87**, 1413–1421 (1991).

33. C. Radmayr, Z. Culig, A. Hobisch, S. Corvin, G. Bartsch, H. Klocker, Analysis of a mutant androgen receptor offers a treatment modality in a patient with partial androgen insensitivity syndrome. *Eur. Urol.* **33**, 222–226 (1998).

34. T. R. Brown, D. B. Lubahn, E. M. Wilson, F. S. French, C. J. Migeon, J. L. Corden, Functional characterization of naturally occurring mutant androgen receptors from subjects with complete androgen insensitivity. *Mol. Endocrinol.* **4**, 1759–1772 (1990).

35. J. M. Lobaccaro, S. Lumbroso, R. Ktari, R. Dumas, C. Sultan, An exonic point mutation creates a *Mae*III site in the androgen receptor gene of a family with complete androgen insensitivity syndrome. *Hum. Mol. Genet.* **2** (1993), pp. 1041–1043.

36. Y.-H. Liu, C. Li, S.-F. Zhou, Prediction of Deleterious Functional Effects of Non-Synonymous Single Nucleotide Polymorphisms in Human Nuclear Receptor Genes Using a Bioinformatics Approach. *Drug Metab. Lett.* **3**, 242–286 (2009).

37. R. Tadokoro-Cuccaro, T. I. Bunch, J. W. Schwabe, I. A. Hughes, J. C. Murphy, Comparison of the molecular consequences of different mutations at residue 754 and 690 of the androgen receptor (AR) and androgen insensitivity syndrome (AIS) phenotype. *Clin. Endocrinol.* **71**, 253–260 (2009).

38. M. Marcelli, M. Ittmann, S. Mariani, R. Sutherland, R. Nigam, L. Murthy, Y. Zhao, D. Diconcini, E. Puxeddu, A. Esen, J. Eastham, N. L. Weigel, D. J. Lamb, Androgen receptor mutations in prostate cancer. *Cancer Res.* **60**, 944–949 (2000).

39. X. B. Shi, A. H. Ma, L. Xia, H. J. Kung, R. W. De Vere White, Functional analysis of 44 mutant androgen receptors from human prostate cancer. *Cancer Res.* **62**, 1496–1502 (2002).

40. X. E. Zhou, K. M. Suino-Powell, J. Li, Y. He, J. P. MacKeigan, K. Melcher, E. L. Yong, H. E. Xu, Identification of SRC3/AIB1 as a preferred coactivator for hormone-activated androgen receptor. *J. Biol. Chem.* **285**, 9161–9171 (2010).

41. S. Grosdidier, L. R. Carbó, V. Buzón, G. Brooke, P. Nguyen, J. D. Baxter, C. L. Bevan, P. Webb, E. Estébanez-Perpiñá, J. Fernández-Recio, Allosteric conversation in the androgen receptor ligand-binding domain surfaces. *Mol. Endocrinol.* **26**, 1078–1090 (2012).

42. C. W. Hay, I. J. McEwan, The impact of point mutations in the human androgen receptor: Classification of mutations on the basis of transcriptional activity. *PLOS ONE* **7**, e32514 (2012).

43. M. J. McPhaul, M. Marcelli, W. D. Tilley, J. E. Griffin, R. F. Isidro-Gutierrez, J. D. Wilson, Molecular basis of androgen resistance in a family with a qualitative abnormality of the androgen receptor and responsive to high-dose androgen therapy. *J. Clin. Invest.* **87**, 1413–1421 (1991).

44. I. Murono, B. B. Mendonca, I. J. Arnhold, A. C. Rigon, C. J. Migeon, T. R. Brown, Human androgen insensitivity due to point mutations encoding amino acid substitutions in the androgen receptor steroid-binding domain. *Hum. Mutat.* **6**, 152–162 (1995).

45. C. A. Quigley, A. De Bellis, K. B. Marschke, M. K. El-Awady, E. M. Wilson, F. S. French, Androgen receptor defects: Historical, clinical, and molecular perspectives. *Endocr. Rev.* **16**, 271–321 (1995).

46. E. Langley, J. A. Kemppainen, E. M. Wilson, Intermolecular NH2−/carboxyl-terminal interactions in androgen receptor dimerization revealed by mutations that cause androgen insensitivity. *J. Biol. Chem.* **273**, 92–101 (1998).

47. K. F. Melo, B. B. Mendonca, A. E. C. Billerbeck, E. M. Costa, M. Inácio, F. A. Silva, A. M. Leal, A. C. Latronico, I. J. Arnhold, Clinical, hormonal, behavioral, and genetic characteristics of androgen insensitivity syndrome in a Brazilian cohort: Five novel mutations in the androgen receptor gene. *J. Clin. Endocrinol. Metab.* **88**, 3241–3250 (2003).

48. I. Jääskeläinen, A. Deeb, J. W. Schwabe, N. P. Mongan, H. Martin, I. A. Hughes, Human androgen receptor gene ligand-binding-domain mutations leading to disrupted interaction between the N- and C-terminal domains. *J. Mol. Endocrinol.* **36**, 361–368 (2006).

49. J. Batch, D. Williams, H. Davies, B. Brown, B. A. Evans, I. A. Hughes, M. Patterson, Androgen receptor gene mutations identified by SSCP in fourteen subjects with androgen insensitivity syndrome. *Hum. Mol. Genet.* **1**, 497–503 (1992).

50. C. L. Bevan, B. B. Brown, H. R. Davies, B. A. Evans, I. A. Hughes, M. N. Patterson, Functional analysis of six androgen receptor mutations identified in patients with partial androgen insensitivity syndrome. *Hum. Mol. Genet.* **5**, 265–273 (1996).

51. Q. Wang, F. J. Ghadessy, A. Trounson, D. de Kretser, R. McLachlan, S. Ng, E. Yong, Azoospermia associated with a mutation in the ligand-binding domain of an androgen receptor displaying normal ligand binding, but defective trans-activation. *J. Clin. Endocrinol. Metab.* **83**, 4303–4309 (1998).

52. O. Hiort, P.-M. Holterhus, T. Horter, W. Schulze, B. Kremke, M. Bals-Pratsch, G. H. G. Sinnecker, K. Kruse, Significance of Mutations in the Androgen Receptor Gene in Males with Idiopathic infertility. *J. Clin. Endocrinol. Metab.* **85**, 2810–2815 (2000).

53. N. Kalfa, P. Philibert, R. Werner, F. Audran, A. Bashamboo, H. Lehors, M. Haddad, J. M. Guys, R. Reynaud, P. Alessandrini, K. Wagner, J. Y. Kurzenne, F. Bastiani, J. Bréaud, J. S. Valla, G. M. Lacombe, M. Orsini, J. P. Daures, O. Hiort, F. Paris, K. McElreavey, C. Sultan, Minor hypospadias: The "Tip of the Iceberg" of the partial androgen insensitivity syndrome. *PLOS ONE* **8**, e61824 (2013).

54. J. Qi, M. Tripathi, R. Mishra, N. Sahgal, L. Fazil, S. Ettinger, W. J. Placzek, G. Claps, L. W. Chung, D. Bowtell, M. Gleave, N. Bhowmick, Z. A. Ronai, The E3 ubiquitin ligase siah2 contributes to castration-resistant prostate cancer by regulation of androgen receptor transcriptional activity. *Cancer Cell* **23**, 332–346 (2013).

55. R. Kumar, J. Mendonca, O. Owoyemi, K. Boyapati, N. Thomas, S. Kanacharoen, M. Coffey, D. Topiwala, C. Gomes, B. Ozbek, T. Jones, M. Rosen, L. Dong, S. Wiens, W. N. Brennen, J. T.

Isaacs, A. M. D. Marzo, M. C. Markowski, E. S. Antonarakis, D. Z. Qian, K. J. Pienta, D. M. Pardoll, M. A. Carducci, S. R. Denmeade, S. K. Kachhap, Supraphysiologic testosterone induces ferroptosis and activates immune pathways through nucleophagy in prostate cancer. *Cancer Res.* **81**, 5948–5962 (2021).

56. H. M. Lam, H. M. Nguyen, M. P. Labrecque, L. G. Brown, I. M. Coleman, R. Gulati, B. Lakely, D. Sondheim, P. Chatterjee, B. T. Marck, A. M. Matsumoto, E. A. Mostaghel, M. T. Schweizer, P. S. Nelson, E. Corey, Durable response of enzalutamide-resistant prostate cancer to supraphysiological testosterone is associated with a multifaceted growth suppression and impaired DNA damage response transcriptomic program in patient-derived xenografts. *Eur. Urol.* **77**, 144–155 (2020).

57. L. Garcia-Alonso, C. H. Holland, M. M. Ibrahim, D. Turei, J. Saez-Rodriguez, Benchmark and integration of resources for the estimation of human transcription factor activities. *Genome Res.* **29**, 1363–1375 (2019).

58. A. Aytes, A. Mitrofanova, C. Lefebvre, M. J. Alvarez, M. Castillo-Martin, T. Zheng, J. A. Eastham, A. Gopalan, K. J. Pienta, M. M. Shen, A. Califano, C. Abate-Shen, Cross-species regulatory Network Analysis identifies a synergistic interaction between FOXM1 and CENPF that drives prostate cancer malignancy. *Cancer Cell* **25**, 638 (2014), 651.

59. H. Takahashi, M. Furusato, W. C. Allsbrook, H. Nishii, S. Wakui, J. C. Barrett, J. Boyd, Prevalence of androgen receptor gene mutations in latent prostatic carcinomas from japanese men. *Cancer Res.* **55**, 1621–1624 (1995).

60. W. Weidemann, B. Linck, H. Haupt, B. Mentrup, G. Romalo, K. Stockklauser, A. O. Brinkmann, H. U. Schweikert, K. D. Spindler, Clinical and biochemical investigations and molecular analysis of subjects with mutations in the androgen receptor gene. *Clin. Endocrinol.* **45**, 733–739 (1996).

61. J. Thompson, F. Saatcioglu, O. A. Jänne, J. J. Palvimo, Disrupted amino- and carboxyl- terminal interactions of the androgen receptor are linked to androgen insensitivity. *Mol. Endocrinol.* **15**, 923–935 (2001).

62. O. A. O'Mahony, M. P. Steinkamp, M. A. Albertelli, M. Brogley, H. Rehman, D. M. Robins, Profiling human androgen receptor mutations reveals treatment effects in a mouse model of prostate cancer. *Mol. Cancer Res.* **6**, 1691–1701 (2008).

63. E. Estébanez-Perpiñá, L. A. Arnold, P. Nguyen, E. D. Rodrigues, E. Mar, R. Bateman, P. Pallai, K. M. Shokat, J. D. Baxter, R. K. Guy, P. Webb, R. J. Fletterick, A surface on the androgen receptor that allosterically regulates coactivator binding. *Proc. Natl. Acad. Sci. U.S.A.* **104**, 16074–16079 (2007).

64. A. Jiménez-Panizo, A. Alegre-Martí, T. T. Tettey, G. Fettweis, M. Abella, R. Antón, T. A. Johnson, S. Kim, R. L. Schiltz, I. Núñez-Barrios, J. Font-Díaz, C. Caelles, A. F. Valledor, P. Pérez, A. M. Rojas, J. Fernández-Recio, D. M. Presman, G. L. Hager, P. Fuentes-Prior, E. Estébanez-Perpiñá, The multivalency of the glucocorticoid receptor ligand-binding domain explains its manifold physiological activities. *Nucleic Acids Res.* **50**, gkac1119 (2022).

65. S. Grosdidier, J. Fernández-Recio, Identification of hot-spot residues in protein-protein interactions by computational docking. *BMC Bioinformatics* **9**, 447 (2008).

66. J. Fernandez-Recio, M. Totrov, C. Skorodumov, R. Abagyan, Optimal docking area: A new method for predicting protein-protein interaction sites. *Proteins* **58**, 134–143 (2005).

67. L. Sun, M. Wang, Z. Lv, N. Yang, Y. Liu, S. Bao, W. Gong, R. M. Xu, Structural insights into protein arginine symmetric dimethylation by PRMT5. *Proc. Natl. Acad. Sci. U.S.A.* **108**, 20538–20543 (2011).

68. S. Antonysamy, Z. Bonday, R. M. Campbell, B. Doyle, Z. Druzina, T. Gheyi, B. Han, L. N. Jungheim, Y. Qian, C. Rauch, M. Russell, J. M. Sauder, S. R. Wasserman, K. Weichert, F. S. Willard, A. Zhang, S. Emtage, Crystal structure of the human PRMT5:MEP50 complex. *Proc. Natl. Acad. Sci. U.S.A.* **109**, 17960–17965 (2012).

69. M. C. Ho, C. Wilczek, J. B. Bonanno, L. Xing, J. Seznec, T. Matsui, L. G. Carter, T. Onikubo, P. R. Kumar, M. K. Chan, M. Brenowitz, R. H. Cheng, U. Reimer, S. C. Almo, D. Shechter, Structure of

the arginine methyltransferase PRMT5-MEP50 reveals a mechanism for substrate specificity. *PLOS ONE* **8**, e57008 (2013).

70. K. M. Mulvaney, C. Blomquist, N. Acharya, R. Li, M. J. Ranaghan, M. O'Keefe, D. J. Rodriguez, M. J. Young, D. Kesar, D. Pal, M. Stokes, A. J. Nelson, S. S. Jain, A. Yang, Z. Mullin-Bernstein, J. Columbus, F. K. Bozal, A. Skepner, D. Raymond, S. LaRussa, D. C. McKinney, Y. Freyzon, Y. Baidi, D. Porter, A. J. Aguirre, A. Ianari, B. McMillan, W. R. Sellers, Molecular basis for substrate recruitment to the PRMT5 methylosome. *Mol. Cell* **81**, 3481–3495.e7 (2021).

71. M. T. Schweizer, E. S. Antonarakis, H. Wang, A. Seun Ajiboye, A. Spitz, H. Cao, J. Luo, M. C. Haffner, S. Yegnasubramanian, M. A. Carducci, M. A. Eisenberger, J. T. Isaacs, S. R. Denmeade, Effect of bipolar androgen therapy for asymptomatic men with castration-resistant prostate cancer: Results from a pilot clinical study. *Sci. Transl. Med.* **7**, 269ra2 (2015).

72. M. D. Nyquist, L. S. Ang, A. Corella, I. M. Coleman, M. P. Meers, A. J. Christiani, C. Pierce, D. H. Janssens, H. E. Meade, A. Bose, L. Brady, T. Howard, N. De Sarkar, S. B. Frank, R. F. Dumpit, J. T. Dalton, E. Corey, S. R. Plymate, M. C. Haffner, E. A. Mostaghel, P. S. Nelson, Selective androgen receptor modulators activate the canonical prostate cancer androgen receptor program and repress cancer growth. *J. Clin. Invest.* **131**, e146777 (2021).

73. X. Qiu, L. G. Brown, J. L. Conner, H. M. Nguyen, N. Boufaied, S. A. Alaiwi, J. H. Seo, T. El Zarif, C. Bell, E. O'Connor, B. Hanratty, M. Pomerantz, M. L. Freedman, M. Brown, M. C. Haffner, P. S. Nelson, F. Y. Feng, D. P. Labbé, H. W. Long, E. Corey, Response to supraphysiological testosterone is predicted by a distinct androgen receptor cistrome. *JCI Insight* **7**, e157164 (2022).

74. V. Sheikhhassani, B. Scalvini, J. Ng, L. W. H. J. Heling, Y. Ayache, T. M. J. Evers, E. Estébanez-Perpiñá, I. J. McEwan, A. Mashaghi, Topological dynamics of an intrinsically disordered N-terminal domain of the human androgen receptor. *Protein Sci.* **31**, e4334 (2022).

75. S. A. Mosure, P. Munoz-Tello, K.-T. Kuo, B. M. Tavish, X. Yu, D. Scholl, C. C. Williams, T. S. Strutzenberg, J. Bass, R. Brust, A. A. Deniz, P. R. Griffin, D. J. Kojetin, Structural basis of interdomain communication in PPARγ (2022); www.biorxiv.org/content/10.1101/2022.07.13.499031v1.abstract.

76. X. Zhang, X. Cheng, Structure of the Predominant Protein Arginine Methyltransferase PRMT1 and Analysis of Its Binding to Substrate Peptides. *Structure* **11**, 509–520 (2003).

77. D. Musiani, J. Bok, E. Massignani, L. Wu, T. Tabaglio, M. R. Ippolito, A. Cuomo, U. Ozbek, H. Zorgati, U. Ghoshdastider, R. C. Robinson, E. Guccione, T. Bonaldi, Proteomics profiling of arginine methylation defines PRMT5 substrate specificity. *Sci. Signal.* **12**, eaat8388 (2019).

78. E. S. Burgos, C. Wilczek, T. Onikubo, J. B. Bonanno, J. Jansong, U. Reimer, D. Shechter, Histone H2A and H4 N-terminal tails are positioned by the MEP50 WD repeat protein for efficient methylation by the PRMT5 arginine methyltransferase. *J. Biol. Chem.* **290**, 9674–9689 (2015).

79. P. Chymkowitch, N. Le May, P. Charneau, E. Compe, J. M. Egly, The phosphorylation of the androgen receptor by TFIIH directs the ubiquitin/proteasome process. *EMBO J.* **30**, 468–479 (2011).

80. S. Sarkar, D. L. Brautigan, S. J. Parsons, J. M. Larner, Androgen receptor degradation by the E3 ligase CHIP modulates mitotic arrest in prostate cancer cells. *Oncogene* **33**, 26–33 (2014).

81. C. Liu, W. Lou, J. C. Yang, L. Liu, C. M. Armstrong, A. P. Lombard, R. Zhao, O. D. V. Noel, C. G. Tepper, H. W. Chen, M. Dall'Era, C. P. Evans, A. C. Gao, Proteostasis by STUB1/HSP70 complex controls sensitivity to androgen receptor targeted therapy in advanced prostate cancer. *Nat. Commun.* **9**, 4700 (2018).

82. M. L. Mohler, A. Sikdar, S. Ponnusamy, D. J. Hwang, Y. He, D. D. Miller, R. Narayanan, An overview of next-generation androgen receptor-targeted therapeutics in development for the treatment of prostate cancer. *Int. J. Mol. Sci.* **22**, 2124 (2021).

83. S. Ha, G. Luo, H. Xiang, A comprehensive overview of small-molecule androgen receptor degraders: Recent progress and future perspectives. *J. Med. Chem.* **65**, 16128–16154 (2022).

84. X. Deng, G. Shao, H. T. Zhang, C. Li, D. Zhang, L. Cheng, B. D. Elzey, R. Pili, T. L. Ratliff, J. Huang, C. D. Hu, Protein arginine methyltransferase 5 functions as an epigenetic activator of the androgen receptor to promote prostate cancer cell growth. *Oncogene* **36**, 1223–1231 (2017).

85. K. Hosohata, P. Li, Y. Hosohata, J. Qin, R. G. Roeder, Z. Wang, Purification and identification of a novel complex which is involved in androgen receptor-dependent transcription. *Mol. Cell. Biol.* **23**, 7019–7029 (2003).

86. Y. Peng, F. Chen, J. Melamed, L. Chiriboga, J. Wei, X. Kong, M. Mcleod, Y. Li, C. X. Li, A. Feng, M. J. Garabedian, Z. Wang, R. G. Roeder, P. Lee, Distinct nuclear and cytoplasmic functions of androgen receptor cofactor p44 and association with androgen-independent prostate cancer. *Proc. Natl. Acad. Sci. U.S.A.* **105**, 5236–5241 (2008).

87. L. Zhou, H. Wu, P. Lee, Z. Wang, Roles of the androgen receptor cofactor p44 in the growth of prostate epithelial cells. *J. Mol. Endocrinol.* **37**, 283–300 (2006).

88. S. Yin, L. Liu, C. Brobbey, V. Palanisamy, L. E. Ball, S. K. Olsen, M. C. Ostrowski, W. Gan, PRMT5-mediated arginine methylation activates AKT kinase to govern tumorigenesis. *Nat. Commun.* **12**, 3444 (2021).

89. C. Helsen, T. Nguyen, T. Vercruysse, S. Wouters, D. Daelemans, A. Voet, F. Claessens, The T850D phosphomimetic mutation in the androgen receptor ligand binding domain enhances recruitment at activation function 2. *Int. J. Mol. Sci.* **23**, 1557 (2022).

90. I. Maksimovic, Y. David, Non-enzymatic covalent modifications as a new chapter in the histone code. *Trends Biochem. Sci.* **46**, 718–730 (2021).

91. H. S. Soifer, N. Souleimanian, S. Wu, A. M. Voskresenskiy, F. K. Collak, B. Cinar, C. A. Stein, Direct regulation of androgen receptor activity by potent CYP17 inhibitors in prostate cancer cells. *J. Biol. Chem.* **287**, 3777–3787 (2012).

92. A. Dobin, C. A. Davis, F. Schlesinger, J. Drenkow, C. Zaleski, S. Jha, P. Batut, M. Chaisson, T. R. Gingeras, STAR: Ultrafast universal RNA-seq aligner. *Bioinformatics* **29**, 15–21 (2013).

93. A. Frankish, M. Diekhans, A. M. Ferreira, R. Johnson, I. Jungreis, J. Loveland, J. M. Mudge, C. Sisu, J. Wright, J. Armstrong, I. Barnes, A. Berry, A. Bignell, S. Carbonell Sala, J. Chrast, F. Cunningham, T. Di Domenico, S. Donaldson, I. T. Fiddes, C. García Girón, J. M. Gonzalez, T. Grego, M. Hardy, T. Hourlier, T. Hunt, O. G. Izuogu, J. Lagarde, F. J. Martin, L. Martínez, S.

Mohanan, P. Muir, F. C. P. Navarro, A. Parker, B. Pei, F. Pozo, M. Ruffier, B. M. Schmitt, E. Stapleton, M. M. Suner, I. Sycheva, B. Uszczynska-Ratajczak, J. Xu, A. Yates, D. Zerbino, Y. Zhang, B. Aken, J. S. Choudhary, M. Gerstein, R. Guigó, T. J. P. Hubbard, M. Kellis, B. Paten, A. Reymond, M. L. Tress, P. Flicek, GENCODE reference annotation for the human and mouse genomes. *Nucleic Acids Res.* **47**, D766–D773 (2019).

94. V. Jimenez-Jacinto, A. Sanchez-Flores, L. Vega-Alvarado, Integrative Differential expression analysis for multiple experiments (IDEAMEX): A web server tool for integrated RNA-seq data analysis. *Front. Genet.* **10**, 279 (2019).

95. M. I. Love, W. Huber, S. Anders, Moderated estimation of fold change and dispersion for RNA-seq data with DESeq2. *Genome Biol.* **15**, 550 (2014).

96. M. E. Ritchie, B. Phipson, D. Wu, Y. Hu, C. W. Law, W. Shi, G. K. Smyth, *limma* powers differential expression analyses for RNA-sequencing and microarray studies. *Nucleic Acids Res.* **43**, e47 (2015).

97. Z. Gu, R. Eils, M. Schlesner, Complex heatmaps reveal patterns and correlations in multidimensional genomic data. *Bioinformatics* **32**, 2847–2849 (2016).

98. S. Anders, W. Huber, Differential expression analysis for sequence count data. *Genome Biol.* **11**, R106 (2010).

99. A. Subramanian, P. Tamayo, V. K. Mootha, S. Mukherjee, B. L. Ebert, M. A. Gillette, A. Paulovich, S. L. Pomeroy, T. R. Golub, E. S. Lander, J. P. Mesirov, Gene set enrichment analysis: A knowledge-based approach for interpreting genome-wide expression profiles. *Proc. Natl. Acad. Sci. U.S.A.* **102**, 15545–15550 (2005).

100. T. Wu, E. Hu, S. Xu, M. Chen, P. Guo, Z. Dai, T. Feng, L. Zhou, W. Tang, L. Zhan, X. Fu, S. Liu, X. Bo, G. Yu, clusterProfiler 4.0: A universal enrichment tool for interpreting omics data. *Innovation* **2**, 100141 (2021).

101. M. Schubert, B. Klinger, M. Klünemann, A. Sieber, F. Uhlitz, S. Sauer, M. J. Garnett, N. Blüthgen, J. Saez-Rodriguez, Perturbation-response genes reveal signaling footprints in cancer gene expression. *Nat. Commun.* **9**, 20 (2018).

102. C. Poulard, J. Jacquemetton, T. H. Pham, M. Le Romancer, Using proximity ligation assay to detect protein arginine methylation. *Methods* **175**, 66–71 (2020).

103. J. Schindelin, I. Arganda-Carreras, E. Frise, V. Kaynig, M. Longair, T. Pietzsch, S. Preibisch, C. Rueden, S. Saalfeld, B. Schmid, J. Y. Tinevez, D. J. White, V. Hartenstein, K. Eliceiri, P. Tomancak, A. Cardona, Fiji: An open-source platform for biological-image analysis. *Nat. Methods* **9**, 676–682 (2012).

104. R. Gustafsson, U. Eckhard, W. Ye, E. D. Enbody, M. Pettersson, P. Jemth, L. Andersson, M. Selmer, Structure and characterization of phosphoglucomutase 5 from atlantic and baltic herring— An inactive enzyme with intact substrate binding. *Biomolecules.* **10**, 1631 (2020).

105. T. M. K. Cheng, T. L. Blundell, J. Fernandez-Recio, PyDock: Electrostatics and desolvation for effective scoring of rigid-body protein-protein docking. *Proteins Struct. Funct. Genet.* **68**, 503–515 (2007).

106. J. Fernández-Recio, M. Totrov, R. Abagyan, Identification of protein-protein interaction sites from docking energy landscapes. *J. Mol. Biol.* **335**, 843–865 (2004).

107. R. Guerois, J. E. Nielsen, L. Serrano, Predicting changes in the stability of proteins and protein complexes: A study of more than 1000 mutations. *J. Mol. Biol.* **320**, 369–387 (2002).

108. N. Halabi, O. Rivoire, S. Leibler, R. Ranganathan, Protein sectors: Evolutionary units of three-dimensional structure. *Cell* **138**, 774–786 (2009).

109. S. W. Lockless, R. Ranganathan, Evolutionarily conserved pathways of energetic connectivity in protein families. *Science* **286**, 295–299 (1999).

110. O. Rivoire, K. A. Reynolds, R. Ranganathan, Evolution-Based Functional Decomposition of Proteins. *PLOS Comput. Biol.* **12**, e1004817 (2016).

111. J. Wang, R. M. Wolf, J. W. Caldwell, P. A. Kollman, D. A. Case, Development and testing of a general Amber force field. *J. Comput. Chem.* **25**, 1157–1174 (2004).

112. C. I. Bayly, P. Cieplak, W. D. Cornell, P. A. Kollman, A well-behaved electrostatic potential based method using charge restraints for deriving atomic charges: The RESP model. *J. Phys. Chem.* **97**, 10269–10280 (1993).

113. S. Izadi, R. Anandakrishnan, A. V. Onufriev, Building water models: A different approach. *J. Phys. Chem. Lett.* **5**, 3863–3871 (2014).

114. C. Tian, K. Kasavajhala, K. A. A. Belfon, L. Raguette, H. Huang, A. N. Migues, J. Bickel, Y. Wang, J. Pincay, Q. Wu, C. Simmerling, Ff19SB: Amino-acid-specific protein backbone parameters trained against quantum mechanics energy surfaces in solution. *J. Chem. Theory Comput.* **16**, 528–552 (2020).

115. T. Darden, D. York, L. Pedersen, Particle mesh Ewald: An $N \cdot \log(N)$ method for Ewald sums in large systems. *J. Chem. Phys.* **98**, 10089–10092 (1993).

116. J. J. Perez, M. S. Tomas, J. Rubio-Martinez, Assessment of the sampling performance of multiple-copy dynamics versus a unique trajectory. *J. Chem. Inf. Model.* **56**, 1950–1962 (2016).

117. C. W. Hopkins, S. Le Grand, R. C. Walker, A. E. Roitberg, Long-time-step molecular dynamics through hydrogen mass repartitioning. *J. Chem. Theory Comput.* **11**, 1864–1874 (2015).

118. J. P. Ryckaert, G. Ciccotti, H. J. C. Berendsen, Numerical integration of the cartesian equations of motion of a system with constraints: Molecular dynamics of n-alkanes. *J. Comput. Phys.* **23**, 327–341 (1977).

119. S. Vatansever, B. Erman, Z. H. Gümüş, Oncogenic G12D mutation alters local conformations and dynamics of K-Ras. *Sci. Rep.* **9**, 11730 (2019).

120. A. R. Atilgan, P. Akan, C. Baysal, Small-world communication of residues and significance for protein dynamics. *Biophys. J.* **86**, 85–91 (2004).

121. Y. C. Yang, C. A. Banuelos, N. R. Mawji, J. Wang, M. Kato, S. Haile, I. J. McEwan, S. Plymate, M. D. Sadar, Targeting androgen receptor activation function-1 with EPI to overcome resistance mechanisms in castration-resistant prostate cancer. *Clin. Cancer Res.* **22**, 4466–4477 (2016).

122. N. G. R. D. Elshan, M. B. Rettig, M. E. Jung, Molecules targeting the androgen receptor (AR) signaling axis beyond the AR-Ligand binding domain. *Med. Res. Rev.* **39**, 910–960 (2019).